T Wegener et al.

Development and Analyses of Self-Passivating Tungsten Alloys for DEMO Accidental Conditions

Development and Analyses of Self-Passivating Tungsten Alloys for DEMO Accidental Conditions

Tobias Wegener[a,*], Felix Klein[a], Andrey Litnovsky[a], Marcin Rasinski[a], Jens Brinkmann[a,b], Freimut Koch[b], Christian Linsmeier[a]

[a]*Forschungszentrum Jülich GmbH, Institut für Energie- und Klimaforschung - Plasmaphysik, Partner of the Trilateral Euregio Cluster (TEC), 52425 Jülich, Germany*
[b]*Max-Planck-Institut für Plasmaphysik, D-85748 Garching*

Abstract

Tungsten is considered the main candidate material for the first-wall in DEMO due to its high melting point, low erosion yield and low tritium retention. Nevertheless, it can cause a substantial safety issue in a loss-of-coolant accident (LOCA) in combination with air ingress into the plasma vessel, due to the formation and evaporation of volatile neutron activated tungsten oxide. Self-passivating tungsten alloys introduce a passive safety mechanism by forming a stable chromic oxide layer on the surface acting as a diffusion barrier for oxygen and preventing the formation of tungsten oxide. Self-passivating tungsten alloys optimized for oxidation resistance containing ~ 11 wt.% chromium and ~ 0.6 wt.% yttrium are investigated under conditions of argon-oxygen, humid argon and humid air atmospheres at different partial pressures and temperatures ranging from 1073–1273 K. Thin films with ~ 3.5 μm thickness produced by magnetron sputtering are used as a model system. The oxidation resistance of theses films in an argon-20 vol.% oxygen atmosphere is sufficient to prevent formation and release of tungsten oxide at temperatures of from 1073–1273 K. The evaporation of chromium in nitrogen-oxygen-water atmosphere at $T \geq 1273$ K is discussed. A deeper understanding of the governing processes for oxygen/chromium diffusion under different atmospheres is gained, supported by SEM/EDX in combination with FIB cross-section and TGA measurements.

Keywords: Tungsten alloy, self-passivating tungsten alloy, W-Cr-Y alloy, humid atmosphere oxidation

1. Introduction

The conditions in a demonstration fusion reactor like DEMO pose a significant challenge for materials [1]. Accordingly, tungsten (W) is considered the main candidate material for the first wall of a future fusion reactor hence, its high melting point, low erosion yield, and low tritium retention [2]. Also, in case of a loss-of-coolant accident in combination with an air-ingress W shows a major safety issue. Caused by its linear or catastrophic oxidation behavior W forms WO_3 which is highly volatile at the predicted temperatures of around 800–1450 K [3]. This could result in the evaporation of several hundred kg h^{-1} of the neutron activated WO_3 [4]. For theses reasons, oxidation of W has to be prevented. In literature typically the application of coatings are applied to prevent W from oxidation in volatilization [5]. However, this is not applicable in a working fusion reactor as all materials facing the plasma are eroded, hence the choice of W due to its low erosion yield. A possible solution for the challenge of oxidation is alloying of tungsten with elements which form a stable oxide-layer on the surface and so preventing the formation of volatile WO_3 as it was proposed and studied in (ref. [6, 7, 8, 9, 10, 11, 4]). After the formation of a continuous oxide layer, the diffusion of oxygen through the growing oxide layer gets the rate determining step

[12]. This is resulting in so called parabolic oxidation which can be given as k_p the parabolic oxidation rate. The previous work [4] concentrated on the optimization of the alloy element content and the corresponding samples were only oxidized in dry argon-20 vol.% oxygen (Ar-20 vol.% O_2) atmospheres over rather short periods of time of about ~ 2 h. In this study the W-Cr-Y alloys are further investigated for longer oxidation times of up to 60 h in dry Ar-20 vol.% O_2 at 1073 K and 1273 K and further for oxidation in Ar-5 vol.% H_2O and air-5 vol.% H_2O at 1273 K. This was performed, to test the actual performance under humid air conditions.

2. Materials and methods of investigations

The samples for this study were produced by magnetron sputtering. The magnetron sputter process was described in [4]. Tungsten, chromium and yttrium targets operate simultaneously. For the deposition process chromium (99.95 wt.%) and tungsten (99.95 wt.%) targets were operated by a DC power supply at 180–275 W and 420–500 W. The yttrium (99.9 wt.%) target was operated with a RF power supply at 140–330 W to achieve reliable deposition rates even at low yttrium concentrations in the alloys. The alloys were deposited on sapphire substrates, as recommended in ref. [6]. They have a diameter of 12 mm and 0.5 mm thickness, the deposited films are ~ 3.5 μm thick. The composition of the samples is determined separately for each process by Wavelength-Dispersive X-Ray

---

*Corresponding author
Email address:* `t.wegener@fz-juelich.de` (Tobias Wegener)

Fluorescence (WDXRF) using a sequential x-ray spectrometer (PW2404, PHILIPS). Oxidation testing was performed in a a symmetrical double-oven thermogravimetric system (TGA) TAG 16 from Setaram. Furthermore, the system is also equipped with the steam generator. Accordingly, it was possible to perform experiments in Ar-5 vol.% H_2O and air-5 vol.% H_2O. All parameter for the different experiments given in Tab: 1.

Table 1: Oxidation gas mixtures and flow rates for the different investigated atmospheres

condition	atmosphere [vol.%]	flow [ml min^{-1}]	p [Pa]
A	Ar-20 O_2	10	10^5
B	Ar-5 H_2O	20	10^5
C	N_2-20 O_2-5 H_2O	20	10^5

Before and after oxidation several analytical techniques like scanning electron microscopy (SEM) in combination with focused ion beam (FIB) cross-sectioning and energy dispersive X-ray spectroscopy (EDX) from Carl Zeiss CrossBeam XB 540, X-ray diffraction (XRD) system from Bruker, were employed to examine the micro structure, homogeneity, elemental composition, and morphology of the alloys and the oxides.

3. Results

3.1. Oxidation in dry atmosphere

In dry Ar-20 vol.% O_2 atmosphere (condition A, Tab. 1) W shows a fast linear (catastrophic) oxidation behavior forming WO_3, which simultaneously evaporates. Further, the W-Cr alloy shows a parabolic behavior for about 15 min then fast mass loss is detected.
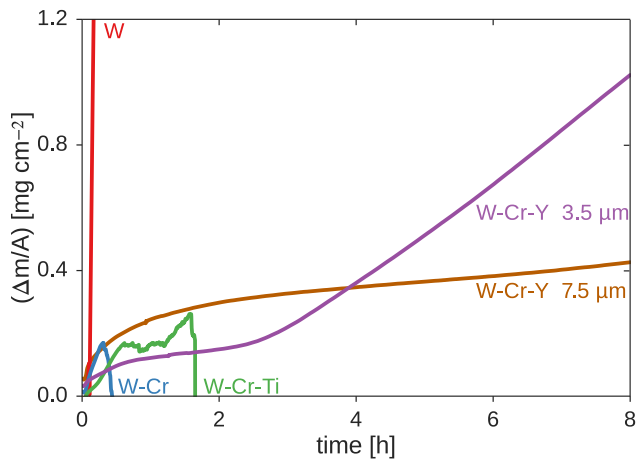

Figure 1: Oxidation of W, W-Cr, W-Cr-Ti and W-Cr-Y in dry Ar-20 vol.%O_2 atmosphere (condition A, Tab. 1) at 1273 K

If about 1 wt.% titanium (Ti) is added to the binary W-Cr the parabolic oxidation behavior is stabilized for up to 30 min. Furthermore, when the Ti is substituted by 0.6 wt.% yttrium (Y) the parabolic behavior is stable for up to 2.5 h at 1273 K and for more than 60 h at 1073 K (see Tab. 2). In addition, for a

film thickness of 7.5 µm this parabolic behavior could even be extended to up to 8.5 h at 1273 K shown in Fig. 1.

Table 2: Measured oxidation constants for different concentrations and thicknesses in dry Ar-20 vol%O_2 atmosphere condition A (Tab. 1).

content [wt.%]	d [µm]	temp. [K]	time [h]	$k_p[\frac{mg^2}{cm^4 s}]$
W-10.5Cr	3.1	1273	0.25	4×10^{-5}
W-10.7Cr-1.1Ti	3.1	1273	0.5	2×10^{-5}
W-11.4Cr-0.6Y	3.3	1273	0.5–2.5	3×10^{-6}
W-13.3Cr-1.0Y	7.5	1273	0.5–8.5	4×10^{-6}
W-13.5Cr-0.4Y	3.5	1073	2–60.0	9×10^{-8}

3.2. Oxidation in humid argon

In humid argon atmosphere condition B (Tab. 1) W shows a slow linear weight increase in Fig. 2. In fact, slower than all other tested materials under theses conditions. W-Cr shows a rather fast but stable parabolic weight increased, the ternary W-Cr-Y on the other hand shows a slower but linear weight gain.
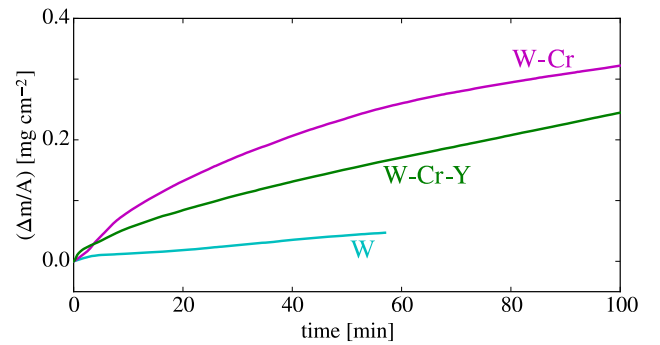

Figure 2: Oxidation of W, W-Cr, and W-Cr-Y in Ar-5 vol.% H_2O atmosphere (condition B, Tab. 1) at 1273 K

3.3. Oxidation in humid air

Under the most challenging of all conditions where humidity and oxygen is combined (compare to C, Tab. 1), W shows an even faster catastrophic oxidation compared to the dry oxygen containing atmosphere case. The short parabolic behavior of W-Cr is further reduced and scale spallation and evaporation occurs. W-Cr-Y shows a ver low weight gain with indications for evaporation (no weight gain or even loss after about 10 min and at the end of the curve in Fig. 3).

3.4. Investigation of oxidation and evaporation in H_2O atmospheres

To investigate, which elements are evaporating, thin-film test samples of pure Cr and W were prepared and oxidized under conditions B and C (Tab. 1). First, the thin films are fully oxidized. Second the weight loss (which is the evaporation) is recorded as shown in Fig. 4. There is no evaporation detectable for pure Cr in humid Ar atmosphere (B, Tab. 1). However, in humid air (C, Tab. 1) evaporation is clearly detectable and has a rate of 5×10^{-6} mg cm^{-2} s^{-1}. Furthermore, pure W shows a one
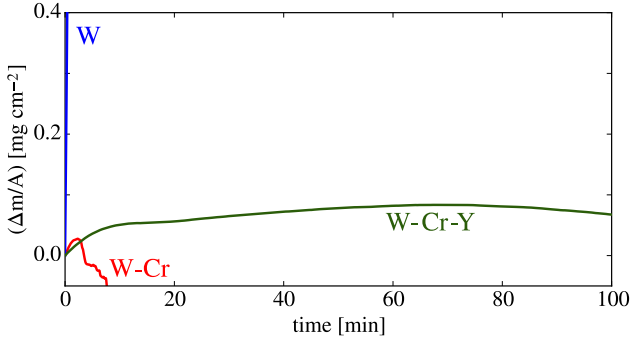
Figure 3: Oxidation of W, W-Cr, and W-Cr-Y in N_2-20 vol.% O_2-5 vol.% H_2O atmosphere (condition C, Tab. 1) at 1273 K

(a) Ar+O_2, 75 min (b) Ar+H_2O, 120 min (c) N_2+O_2+H_2O, 75 min

Figure 5: FIB cross-sections of W-Cr-Y thin-film alloys (a) after 75 min oxidation in Ar-20 vol.% O_2 atmosphere (A, Tab. 1), (b) after 120 min oxidation in Ar-5 vol.% H_2O (B, Tab. 1), and (c) after 75 min oxidation in (C, Tab. 1) at 1273 K

order of magnitude higher evaporation rate 7×10^{-5} mg cm^{-2} s^{-1} under the same conditions.
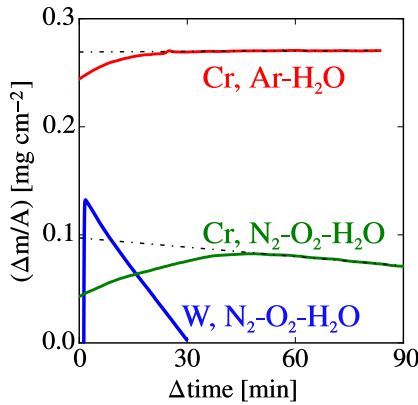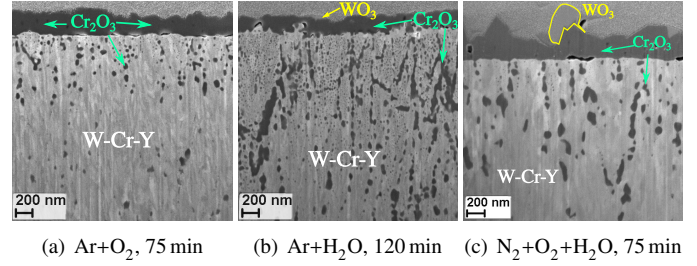

Figure 4: Evaporation after oxidation of pure Cr in Ar-5 vol.% H_2O and N_2-20 vol.% O_2-5 vol.% H_2O (conditions B + C, Tab. 1) and for pure W in N_2-20 vol.% O_2-5 vol.% H_2O (conditions C, Tab. 1)

To compare the differences in the formed oxide-layers caused by the different atmospheres on the W-Cr-Y alloy, focused ion beam cross-sections were prepared as shown in Fig. 5. In the Fig. 5(a) a thick and dense protective Cr_2O_3 layer on top is visible, with no indications for WO_3 and just minor internal oxidation in the alloy (dark spots) which was formed under the atmospheric condition A, Tab. 1. This sample corresponds to the 3.5 μm thick W-Cr-Y samples in Fig. 1, for which the oxidation was stopped at 75 min to investigated the favored stable parabolic oxidation behavior.

In the Fig. 5(b) huge amounts of internal oxidation are visible, the surface oxide layer is thinner than in Fig.5(a) even so the oxidation time was increased from 75 min to 120 min and so most of the weight gain (depicted in the curve W-Cr-Y in Fig. 2) was caused by internal oxidation in humid argon (B. Tab.1). In addition, small amounts of WO_3 are detected on the surface as a light spot on the very surface of the oxide.

In the cross-section of Fig. 5(c) an identical period of 75 min was chosen as for the oxidation in dry Ar-20 vol.% O_2 case. The oxidation is following the depicted curve of W-Cr-Y alloy in Fig. 3. The oxide layer on the surface similarly thick as for the dry oxidation, but it is to note that also WO_3 was formed at the surface. Furthermore, the internal oxidation is slightly more

pronounced than in case of the dry Ar-O_2 oxidation.

4. Discussion

The W-Cr-Y alloy in the Fig. 5(a) shows a kind of ideal oxidation behavior as:

- main mechanism formation of a thick and dense protective Cr_2O_3 layer → parabolic oxidation

- no indications for WO_3 formation

- minor internal oxidation visible in the cross-section (dark spots)

On the contrary in Fig. 5(b) the internal oxidation is the dominant process. This could be caused by a different diffusion and adsorption mechanism. As, Cr_2O_3 forms an ionic lattice so the only probable transport is the diffusion of ions through the oxide layer [12]. Further that means, O_2 and H_2O have to first absorb to the surface to form ions by electron exchange. This is more feasible for the H_2O, as it forms thermodynamically more stable ions by $2\,H_2O + 2\,e^- \rightleftharpoons H_2 + 2\,OH^-$ with less charge, distributed on a bigger ion compared to ($O_2 + 4\,e^- \rightleftharpoons O^{2-}$) the double charged O^{2-} ion. Altogether, this could lead to a faster adsorption and than diffusion of oxygen, in form of OH^- ions through the Cr_2O_3 layer.

Furthermore, the increased amount of hydrogen interstitials originating from ($4\,Cr + 6\,OH^- \rightleftharpoons 2\,Cr_2O_3 + 3\,H_2$) at the metal-oxygen interface could expand the W lattice sufficiently so that the diffusivity of oxygen interstitials is increased (as discussed for steels in [13]). This could explain the higher internal oxidation in both humid atmospheres (B and C, Tab. 1. For the case of the combination of humidity and oxygen (C, Tab. 1) the initial partial pressure of oxygen (p_{O_2}) is significantly higher so the formation of Cr_2O_3 is faster in addition the diffusion of the OH^- is added so we see a similar behavior on the surface rather thick Cr_2O_3 layer and a increased amount of internal oxidation compared to dry Ar-20 vol.% O_2. The formation of WO_3 could be correlated to the additional increased p_{O_2} at the oxide metal interface, which would make it possible that also W^{x+} ions form and diffuse to the surface to form WO_3.

3

5. Summary

Overall the oxidation in dry atmosphere as depicted in Fig. 1 is very promising and shows for the W-Cr-Y system the favorable parabolic oxidation behavior. The end of this behavior seems to be correlated with the exhaustion of the Cr reservoir as it was already discussed in ref [4]. Accordingly, it is shown that the time in which parabolic oxidation takes place could be increased by simply increasing the thickness and thereby the Cr reservoir of the alloy (7.5 µm curve Fig.1). In addition, for a future fusion reactor like DEMO the first-wall armor thickness is for seen to be in the order of ~ 2 mm [1]. It seems probable that this thickness would be sufficient to stay in the parabolic oxidation behavior for a full period of a loss-of-coolant accident. However, the performance of the W-Cr-Y in humid atmosphere have to be improved drastically as evaporation of neutron activated Cr and especially W have to be prevented under all circumstances. One way to improve the situation, at least for Cr is to alloy small amounts of manganese (Mn), as it is done for alloys directly developed to reduce the Cr evaporation [13]. This and the production of bulk test alloys will be subject in future studies.

Acknowledgements

References

[1] Y. Igitkhanov, B. Bazylev, I. Landman, R. Fetzer, Design strategy for the pfc in DEMo reactor, KIT SCIENTIFIC REPORTS (Report-Nr. KIT-SR 7637).

[2] H. Bolt, V. Barabash, G. Federici, J. Linke, A. Loarte, J. Roth, K. Sato, Plasma facing and high heat flux materials - needs for ITER and beyond, Journal of Nuclear Materials 307 - 311, Part 1 (2002) 43–52. doi:10.1016/S0022-3115(02)01175-3.

[3] D. Maisonnier, P. I. Cook, R. A. Sardain, L. D. Pace, R. Forrest, L. Giancarli, S. Hermsmeyer, P. Norajitra, N. Taylor, D. Ward, A Conceptual Study of Commercial Fusion Power Plants, Final Report of the European Fusion Power Plant Conceptual Study (PPCS) EFDA(05)-27/4.10, EFDA (Apr. 2005).

[4] T. Wegener, F. Klein, A. Litnovsky, M. Rasinski, F. K. J. Brinkmann and, C. Linsmeier, Development of yttrium-containing self-passivating tungsten alloys for future fusion power plants, Nuclear Materials and Energy-doi:doi.org/10.1016/j.nme.2016.07.011.

[5] H. J. Nolting, R. A. Jefferys, Oxidation resistant high temperature protective coatings for tungsten, Tech. Rep. ML-TDR-6A-227, Air Force Materials Laboratory Research and Technical Division Air Force Systems Command Wright-Patterson Air Force Base, Ohio, www.dtic.mil/cgi-bin/GetTRDoc?Location=U2&doc=GetTRDoc.pdf&AD=AD0608510 (Jul. 1964).

[6] F. Koch, S. Koeppl, H. Bolt, Self passivating W-based alloys as plasma-facing material, J. Nucl. Mater. 386 - 388 (2009) 572–574, MaterialsProceedings of the Thirteenth International doi:10.1016/j.jnucmat.2008.12.179.

[7] T. Weissgaerber, B. Kloeden, B. Kieback, Self-passivating tungsten alloys, Powder Metallurgy World Congress & Exhibition 3 (2010) 377–383, iSBN: 978-1-899072-12-5.

[8] F. Koch, J. Brinkmann, S. Lindig, T. P. Mishra, C. Linsmeier, Oxidation behaviour of silicon-free tungsten alloys for use as the first wall material, Phys. Scr. 2011 (T145) (2011) 014019. URL http://stacks.iop.org/1402-4896/2011/i=T145/a=014019

[9] S. Telu, A. Patra, M. Sankaranarayana, R. Mitra, S. Pabi, Microstructure and cyclic oxidation behavior of W-Cr alloys prepared by sintering of mechanically alloyed nanocrystalline powders, International Journal of Refractory Metals and Hard Materials 36 (0) (2013) 191–203, Materials¡/ce:title¿. doi:10.1016/j.ijrmhm.2012.08.015.

[10] S. Telu, R. Mitra, S. K. Pabi, Effect of Y_2O_3 addition on oxidation behavior of W-Cr alloys, Metallurgical and Materials Transactions A 46 (12) (2015) 5909–5919. doi:10.1007/s11661-015-3166-z.

[11] A. Calvo, N. Ordás, I. Iturriza, F. Koch, H. Greuner, G. Pintsuk, C. Sarbu, C. García-Rosales, Manufacturing AND testing of self-passivating tungsten alloys of different composition, Nuclear Materials and Energy.

[12] N. Birks, G. Meier, F. Pettit, Introduction to the High-Temperature Oxidation of Metals, Cambridge University Press, 2006.

[13] W. J. Quadakkers, J. Zurek, Oxidation in steam and steam/hydrogen environments, Shreir's Corrosion 1 (2010) 407–456.